Discrete Vortex Representation of Magnetohydrodynamics

R. Kinney,* T. Tajima, and N. Petviashvili
Institute for Fusion Studies, The University of Texas at Austin, Austin, Texas 78712

J. C. McWilliams
National Center for Atmospheric Research, P.O. Box 3000, Boulder, Colorado 80307
(Received 16 October 1992)

We present an alternative approach to statistical analysis of an intermittent ideal magnetohydrodynamics fluid in two dimensions, based on the hydrodynamic discrete vortex model applied to the Elsasser variables. The model contains negative temperature states which predict the formation of magnetic islands, but also includes a natural limit under which the equilibrium states revert to the familiar twin-vortex states predicted by hydrodynamic turbulence theories. Numerical dynamical calculations yield equilibrium spectra in agreement with the theoretical predictions.

PACS numbers: 47.65.+a, 52.30.−q, 52.65.+z

Statistical theories of continuous fluids usually are based on some discrete representation of the fluid. Even though such fluids are not in thermodynamic equilibrium at the molecular level, one can expect real systems to tend towards the statistically favored states during time scales for which the model is valid. For numerical simulation, of course, some discretization of a continuous system is always necessary.

Hydrodynamic turbulence has been discretized by two methods: a truncated Fourier representation, and a point vortex representation. An analytic statistical Fourier analysis has already been applied to two-dimensional magnetohydrodynamics (MHD) [1]. In this Letter, we show that a point-vortex discretization like that used in hydrodynamics (or the equivalent guiding-center plasma [2]) is also possible for 2D MHD, and we give results of statistical analysis as well as direct numerical simulation of the vortex system.

Why is such an approach worth taking? It has been asserted [3] that different approaches to discretization of functional integrations cannot in general be expected to yield equivalent results. Indeed, in the hydrodynamic studies, the two different discretization approaches, while both making similar qualitative predictions about a cascade of energy to low wave numbers, do not yield the same results [4]. A neutral 2D fluid with small dissipation is known to form intermediate-scale vorticity distributions, or coherent structures [5], which dominate the nonlinear evolution. Statistical theories based on inviscid equations [6,7] predict evolutionary tendencies suggestive of such structures, although they cannot complete the fully dissipative formation process. Vortices have nevertheless been taken as a starting point for a large body of work (Refs. [8–12] and many others). The end states predicted by such models have been observed in direct numerical simulation of the primitive fluid equations [13], and the dynamical approach to the end state is well described by a modified vortex model [14]. These successes encourage the search for an analogous approach in 2D MHD. Computationally, discrete-vortex models can qualitatively reproduce the behavior of the primitive fluid equations at a lower cost than a spectral or grid point code [15], and allow the possibility of modeling more general large-scale filamentary structures [16,17]. Taking an analogous approach to MHD simulations could lead to similarly efficient numerical models of magnetic turbulence.

There is mounting observational evidence of intermittent plasma structures occurring in high-β astrophysical plasmas [18]. A high-β plasma, in which the fluid pressure dominates the magnetic pressure, seems likely to form coherent structures in both vorticity and current, and singularities have in fact been predicted in 2D MHD [19], while high-resolution 2D MHD simulations have displayed strongly intermittent states [20]. This evidence adds to our confidence that a treatment of plasma turbulence based on coherent structures will prove to be appropriate.

Long ago, Elsasser [21] pointed out that the basic equations of ideal MHD for an incompressible fluid can be written in the form

$$\frac{\partial \mathbf{u}}{\partial t}+(\mathbf{w}\cdot\nabla)\mathbf{u}=-\nabla\eta,\quad \mathbf{u}=v+\mathbf{B},$$
$$\frac{\partial \mathbf{w}}{\partial t}+(\mathbf{u}\cdot\nabla)\mathbf{w}=-\nabla\eta,\quad \mathbf{w}=\mathbf{v}-\mathbf{B}, \tag{1}$$
$$\nabla\cdot\mathbf{u}=\nabla\cdot\mathbf{w}=0,\quad \eta=p+\tfrac{1}{2}\mathbf{B}^2.$$

Velocities are measured in units of an arbitrary constant v_0, and the magnetic field is measured in units of $B_0=\sqrt{4\pi\rho v_0^2}$. Let us also define functions $\boldsymbol{\Omega}$ and $\mathbf{A}$ by

$$\boldsymbol{\Omega}^u=\nabla\times\mathbf{u},\quad \mathbf{u}=\nabla\times\mathbf{A}^u,\quad \boldsymbol{\Omega}^w=\nabla\times\mathbf{w},\quad \mathbf{w}=\nabla\times\mathbf{A}^w, \tag{2}$$

and choose a gauge in which $\nabla\cdot\mathbf{A}^u=\nabla\cdot\mathbf{A}^w=0$. We will use a species superscript to indicate u or w, or omit any superscript to indicate both possibilities generically.

In a neutral fluid, the vorticity is conservatively advected through the fluid. We seek an analogous result for our Ω's by taking the curl of Eq. (1). The divergence of Eq. (1) gives an equation for the pressure, which can be

0031-9007/93/71(11)/1712(4)$06.00

solved once the fields are known. Defining the differential operators

$$D^u\mathbf{V}\equiv\partial_t\mathbf{V}-\nabla\times(\mathbf{u}\times\mathbf{V}),$$
$$D^w\mathbf{V}\equiv\partial_t\mathbf{V}-\nabla\times(\mathbf{w}\times\mathbf{V}), \tag{3}$$

the curl of the momentum equation becomes

$$D^u\boldsymbol{\Omega}^w+D^w\boldsymbol{\Omega}^u=0, \tag{4}$$

while the curl of the induction equation may be written

$$D^w\boldsymbol{\Omega}^u-D^u\boldsymbol{\Omega}^w=2\mathbf{S}, \tag{5}$$

in which there is a source term

$$\mathbf{S}=\boldsymbol{\Omega}^w\times\boldsymbol{\Omega}^u+\boldsymbol{\Omega}^w\cdot\nabla\mathbf{u}-\boldsymbol{\Omega}^u\cdot\nabla\mathbf{w}$$
$$+\tfrac{1}{2}[\nabla^2(\mathbf{u}\times\mathbf{w})-(\nabla^2\mathbf{u})\times\mathbf{w}-\mathbf{u}\times(\nabla^2\mathbf{w})]. \tag{6}$$

In two dimensions, $\boldsymbol{\Omega}=\Omega\hat{\mathbf{z}}$ and $\mathbf{A}=A\hat{\mathbf{z}}$, and most of the terms in $\mathbf{S}$ vanish identically. What remains can be expressed in terms of the strain rates, $\sigma_1^s\equiv(\partial_x^2-\partial_y^2)A^2$, $\sigma_2^s\equiv\partial_x\partial_yA^s$, and $\sigma^{s2}\equiv\sigma_1^{s2}+\sigma_2^{s2}$:

$$S=\sigma_1^u\sigma_2^w-\sigma_2^u\sigma_1^w. \tag{7}$$

An upper bound for the magnitude of S is therefore

$$|S|\le\sigma^u\sigma^w. \tag{8}$$

Let our plasma consist of a number of u and w filaments with positions $\{\mathbf{x}_i^s\}$ and intensities $\{\alpha_i^s\}$ such that the Ω's then take the form

$$\Omega^s=\sum_i\alpha_i^s\delta(\mathbf{x}-\mathbf{x}_i^s). \tag{9}$$

The variables $\{\mathbf{x}_i^s\}$ and $\{\alpha_i^s\}$ fully determine the fields $\mathbf{u}$, $\mathbf{w}$, and S through Eqs. (9), (2), and (7). Equations (4) and (5) are solved by the motion of the filaments if

$$\frac{d\mathbf{x}_i^u}{dt}=\mathbf{w}(\mathbf{x}_i^u),\quad\frac{d\alpha_i^u}{dt}=S(\mathbf{x}_i^u),$$
$$\frac{d\mathbf{x}_i^w}{dt}=\mathbf{u}(\mathbf{x}_i^w),\quad\frac{d\alpha_i^w}{dt}=-S(\mathbf{x}_i^w). \tag{10}$$

The induction of current represented by the source term is manifested by a simultaneous change (in opposite directions) in the strength of the u and w filaments. The fact that u and w filaments are not necessarily coincident and that filaments are not guaranteed to be present wherever S is nonzero makes this discretization incomplete but probably adequate for large number densities of filaments.

The $\mathbf{u}$ or $\mathbf{w}$ field of an axisymmetric filament falls off as $1/r$, whereas the rate of strain σ^s goes like $1/r^2$. The magnitude of S, therefore, is smaller than the advective term by at least the ratio of a filament's size to the typical filament separation. In the present treatment of zero-sized filaments, we will neglect S entirely, so that the filament strengths α_i^s are constant in time. In our model, then, the sum (or difference) of vorticity and current is pointwise conservatively advected, with the advecting field being $\mathbf{w}$ for a u filament and $\mathbf{u}$ for a w filament. We will later present a more extensive treatment that includes $S\neq0$ and three-dimensional solutions. The former supports the $S=0$ approximation for many aspects of the statistical behavior.

Let us suppose we have, in a box of volume V, N total filaments, N_u of type u and N_w of type w, in which the u's have strength $\pm\alpha^u$ and w's have strength $\pm\alpha^w$. This system of filaments is Hamiltonian with canonical variables $(x_i^s,|\alpha_i^s|y_i^s)$. The (x_i,y_i) are periodic Cartesian coordinates of the ith filament. The Hamiltonian is

$$H(\mathbf{x}_1,\ldots,\mathbf{x}_N)=-\sum_{i\in u}\sum_{j\in w}\alpha_i\alpha_jG(\mathbf{x}_i|\mathbf{x}_j), \tag{11}$$

where $\nabla^2G(\mathbf{x}|\mathbf{x}')=\delta(\mathbf{x}-\mathbf{x}')$, with appropriate boundary conditions. In an infinite domain, $G(\mathbf{x}|\mathbf{x}')\propto\ln|\mathbf{x}-\mathbf{x}'|$. Note also that

$$\int\mathbf{u}\cdot\mathbf{w}=\int A^u\Omega^w=\int A^w\Omega^u=H. \tag{12}$$

The Hamiltonian is the quantity $\int\mathbf{v}^2-\mathbf{B}^2$. By neglecting S, we are doing work by maintaining a constant current along each filament. Thus, the interaction energy of two current filaments is $-\int\mathbf{B}^2$, and the total interaction energy of the system is $\int\mathbf{v}^2-\mathbf{B}^2$, or H. It is perhaps more convenient, however, to view H as a parameter that measures whether the fluid is kinetically or magnetically dominated. Unlike the usual plasma β, which measures the ratio of magnetic energy to microscopic, thermal energy, H measures the difference between the magnetic energy and the kinetic energy due to macroscopic fluid motion. We denote the constant, numerical value of the Hamiltonian by E.

There is a symmetry about $E=0$. The sign of E can be changed by reversing the sign of either of the two fields. The transformation $\mathbf{w}\to-\mathbf{w}$ implies $\mathbf{v}\to\mathbf{B}$ and $\mathbf{B}\to\mathbf{v}$, while $\mathbf{u}\to-\mathbf{u}$ implies $\mathbf{v}\to-\mathbf{B}$ and $\mathbf{B}\to-\mathbf{v}$. Thus, all results obtained for $E>0$ are applicable for $E<0$ with $\mathbf{v}^2\leftrightarrow\mathbf{B}^2$. This symmetry was confirmed in our numerical simulations.

Taking a microcanonical ensemble, the structure function may be calculated explicitly, as was done for a guiding-center plasma [22],

$$\Phi(E,V,N)=\int\delta(E-H(\{\mathbf{x}_i\}))\prod_i d\mathbf{x}_i$$
$$=\frac{1}{2\pi}\int d\lambda\,e^{i\lambda(E-H)}J\prod_{\mathbf{k}}d\rho_u\,d\rho_w+O(N^{-1}). \tag{13}$$

We have invoked the "random-phase approximation" [23] by changing the variables of integration from the filament positions $\mathbf{x}_i$ to the Fourier-transformed filament "charge" densities, $\rho_u(\mathbf{k})$ and $\rho_w(\mathbf{k})$. Ignoring small-scale correlations between the filament positions gives a Jacobian, J, which is simply a product of Gaussians in the ρ's.

The result is that

$$\tilde{\Phi}=\frac{1}{2\pi}\int dz\, e^{iz\tilde{E}}\prod_{n_x,n_y}\left[1+\frac{z^2}{\pi^2\kappa^4}\right]^{-1}, \tag{14}$$

in terms of dimensionless quantities

$$\tilde{\Phi}=\Phi\frac{\sqrt{N_uN_w}\alpha_u\alpha_w}{V^N},\quad \tilde{E}=\frac{E}{\sqrt{N_uN_w}\alpha_u\alpha_w}, \tag{15}$$

where $\kappa^2=n_x^2+n_y^2$ is the dimensionless wave number, and $k^2=(4\pi^2/V)\kappa^2$. The product in the integrand runs over all $n_x,n_y\geq 0$ except $n_x=n_y=0$, and the integral can be reduced to an infinite sum over residues, which occur along the imaginary axis at $z=\pm i\pi\kappa$. Unlike the hydrodynamic structure function, $\tilde{\Phi}$ is symmetric with respect to $\tilde{E}$, and differs from a Gaussian distribution, approaching $e^{-\pi\kappa_{\min}|\tilde{E}|}$ as $\tilde{E}\rightarrow\pm\infty$. Figure 1 shows $\tilde{\Phi}$, from a numerical evaluation of Eq. (14), along with a Gaussian for comparison. Both are normalized to integrate to 1. Also shown are histogram data of $\tilde{E}$ from an ensemble of vortex systems with fixed filament intensities and random filament positions. The small number of events in the tails of the distribution of $\tilde{E}$ cause some scatter in the data, but the data conform to the calculated structure function in the center and clearly deviate from a Gaussian in the tail. Tokamak experiments have measured deviations from Gaussian probability distributions, which have been taken as indicators of intermittency in the turbulent edge plasma [24].

One may also calculate the filament density spectra,

$$\frac{\langle|\rho_u(\kappa)|^2\rangle}{N_u\alpha_u^2}=\frac{\langle|\rho_w(\kappa)|^2\rangle}{N_w\alpha_w^2}=\frac{1}{V^2}\frac{1}{2\pi\tilde{\Phi}}\int dz\, e^{iz\tilde{E}}\left[1+\frac{z^2}{\pi^2\kappa^4}\right]^{-1}\prod_{n_x',n_y'}\left[1+\frac{z^2}{\pi^2\kappa'^4}\right]^{-1}, \tag{16}$$

and the cross-correlation spectrum,

$$\frac{\langle\rho_u(\kappa)\rho_w^*(\kappa)\rangle}{\sqrt{N_uN_w}\alpha_u\alpha_w}=\frac{1}{V^2}\frac{1}{2\pi\tilde{\Phi}}\int dz\,\frac{-iz}{\pi\kappa^2}e^{iz\tilde{E}}\left[1+\frac{z^2}{\pi^2\kappa^4}\right]^{-1}\prod_{n_x',n_y'}\left[1+\frac{z^2}{\pi^2\kappa'^4}\right]^{-1}. \tag{17}$$

Ensemble-averaged spectra of vorticity, $\omega\equiv\hat{\mathbf{z}}\cdot\nabla\times\mathbf{v}$, current, $J\equiv\hat{\mathbf{z}}\cdot\nabla\times\mathbf{B}$, and cross helicity, $\mathbf{v}\cdot\mathbf{B}$, can be calculated by the following relations:

$$\begin{aligned}\langle\omega^2(\kappa)\rangle&=\tfrac{1}{4}\langle|\rho_u(\kappa)+\rho_w(\kappa)|^2\rangle,\\ \langle J^2(\kappa)\rangle&=\tfrac{1}{4}\langle|\rho_u(\kappa)-\rho_w(\kappa)|^2\rangle,\\ \langle\mathbf{v}(\kappa)\cdot\mathbf{B}(\kappa)\rangle&=\kappa^{-2}\tfrac{1}{2}[\langle|\rho_u(\kappa)|^2\rangle-\langle|\rho_w(\kappa)|^2\rangle].\end{aligned} \tag{18}$$

We let $N_u\alpha_u^2=N_w\alpha_w^2\equiv N\alpha^2$, so that $\langle\mathbf{v}\cdot\mathbf{B}\rangle=0$. Regardless of $\tilde{E}$, $\langle\omega^2(\kappa\rightarrow\infty)\rangle=\langle J^2(\kappa\rightarrow\infty)\rangle=\frac{1}{2}N\alpha^2/V^2$. The longest wavelength modes have asymptotic behaviors $\langle\omega^2(\kappa_{\min})\rangle\rightarrow|\tilde{E}|N\alpha^2/V^2$, $\langle J^2(\kappa_{\min})\rangle\approx 0.26N\alpha^2/V^2$ for $\tilde{E}\rightarrow+\infty$, and $\langle\omega^2(\kappa_{\min})\rangle\approx 0.26N\alpha^2/V^2$, $\langle J^2(\kappa_{\min})\rangle\rightarrow|\tilde{E}|N\alpha^2/V^2$ for $\tilde{E}\rightarrow-\infty$. The discrete vortex model, thus, predicts a large-scale vortex dipole when $\tilde{E}\gg 1$, and a large-scale magnetic dipole when $\tilde{E}\ll -1$.

Figure 2 shows the spectra of ω^2 and J^2, with $\tilde{E}=2$. The solid and dashed lines are calculated from numerical integrations of Eqs. (16), (17), and (14). The data points are time averages from a dynamical simulation of Eqs. (9) and (10) using a two-dimensional guiding-center particle-in-center algorithm [25], modified to account for two species of filaments. The peak of $\langle\omega^2\rangle$ at $\kappa_{\min}$ is indicative of the large-scale vortex dipole formed. Figure 3 shows the values of the lowest-wave-number modes, $\langle\omega^2(\kappa_{\min})\rangle$ and $\langle J^2(\kappa_{\min})\rangle$, for positive values of $\tilde{E}$, com-

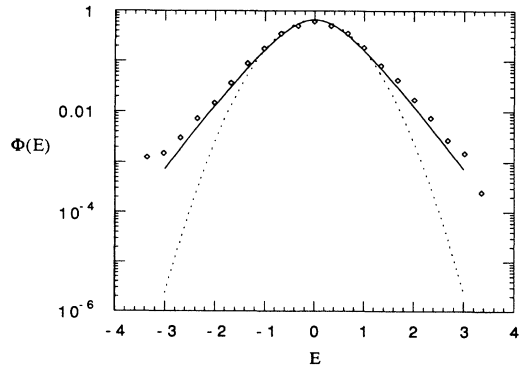

FIG. 1. Structure function $\tilde{\Phi}$, showing phase-space probability density as a function of the energy $\tilde{E}$. Solid line is computed from Eq. (14), and data points are measured histogram frequencies from a set of random configurations. The dotted line is a normalized Gaussian chosen to match at $\tilde{E}=0$, shown for comparison.

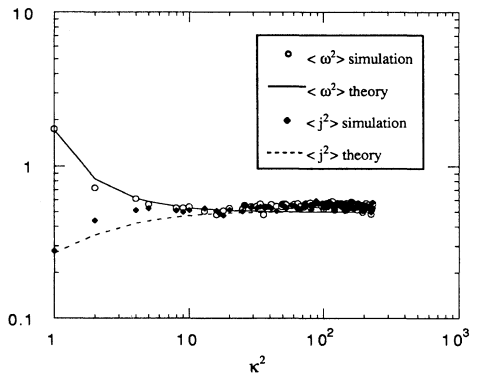

FIG. 2. $\langle J^2\rangle$ and $\langle\omega^2\rangle$ spectra for $\tilde{E}=2$. Data points are time averaged from a dynamical simulation. Solid and dashed lines are spectra predicted from the microcanonical ensemble.

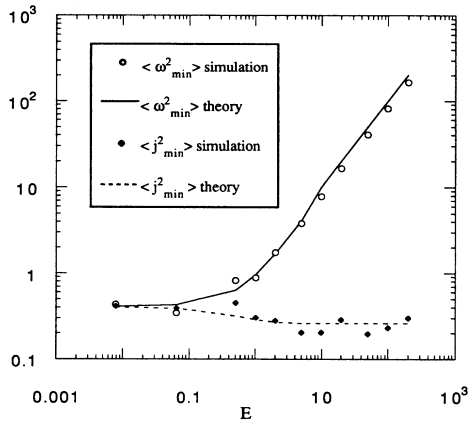

FIG. 3. Values of the lowest-wave-number mode vs $\tilde{E}$ from dynamical runs and theoretical predictions.

paring a series of dynamical runs with the theoretical predictions. The asymptotic behaviors $\langle\omega^2(\kappa_{\min})\rangle \propto \tilde{E}$ and $\langle J^2(\kappa_{\min})\rangle \rightarrow$ const are clearly demonstrated. The corresponding behavior $\langle\omega^2\rangle \leftrightarrow \langle J^2\rangle$ for $\tilde{E} \leftrightarrow -\tilde{E}$ was confirmed, although these results are not shown here.

The above behavior of $\langle J(k_{\min})\rangle$ for $B^2 \gg v^2$ is consistent with results from the truncated Fourier canonical ensemble analysis of [1]. There, $\int v^2 - B^2$ is identified as a parameter whose sign determines whether the magnetic field will peak at long wavelengths, and this peak is proportional to the total energy, as we have found. The spectra differ at large k, however, with the truncated Fourier model predicting $\langle J^2(k \rightarrow \infty)\rangle \propto k^2$.

In the small magnetic field limit, the truncated Fourier and discrete vortex models differ more profoundly. In a neutral fluid, when the kinetic energy is large, Fourier and vortex models both predict a large-scale vortex dipole, with an enstrophy spectrum $\langle\omega^2\rangle$ that has a sharp peak at $k_{\min}$, whose strength is proportional to the kinetic energy [4,22]. This behavior is represented in the $\tilde{E} \gg 1$ state of our model, but the truncated Fourier analysis of MHD predicts no such peak, i.e., $\langle\omega^2(k)\rangle \propto k^2$ in all cases (when $\langle \mathbf{v}\cdot\mathbf{B}\rangle = 0$). The reason is that the Fourier statistics are based on the MHD invariants, but as the magnetic field shrinks to zero, the invariants of the system change. The total energy becomes the kinetic energy normally, but the mean squared magnetic potential goes to zero. The enstrophy, meanwhile, changes at a rate proportional to the magnetic field strength. As the magnetic energy vanishes, any canonical ensemble treatment (like the truncated Fourier representation) should include the enstrophy as an invariant. The omission of the enstrophy changes the spectrum from one with negative temperatures and large-scale structure to a flat equipartition [4].

While two-dimensional MHD possesses an infinity of ideal invariants, and three which survive Fourier truncation, care must be taken in using these as a basis for a statistical analysis. For weak magnetic fields, the enstrophy will also be nearly invariant, and dissipation ultimately destroys all invariants in any case. While we also expect that the effects of neglecting the sources in Eq. (5) will make themselves felt eventually, we have hope that a filamentary representation of MHD, by avoiding explicit reference to inviscid invariants, can avoid some of the above difficulties, particularly those arising from a small magnetic field.

This work was supported by the National Science Foundation and the U.S. Department of Energy.

*Present address: Advanced Study Program, National Center for Atmospheric Research, Boulder, CO 80307.

[1] D. Fyfe and D. Montgomery, J. Plasma Phys. **16**, 181 (1976).
[2] J. B. Taylor and B. McNamara, Phys. Fluids **14**, 1492 (1971).
[3] A. Royer, J. Math. Phys. **25**, 2873 (1984).
[4] R. H. Kraichnan and D. Montgomery, Rep. Prog. Phys. **45**, 547 (1980).
[5] J. C. McWilliams, J. Fluid Mech. **146**, 21 (1984).
[6] R. Robert and J. Sommeria, J. Fluid Mech. **229**, 291 (1991).
[7] J. Miller, Phys. Rev. Lett. **64**, 2137 (1990).
[8] J. M. Kosterlitz, J. Phys. C **7**, 1046 (1974).
[9] T. S. Lundgren and Y. B. Pointin, Phys. Fluids **20**, 356 (1977).
[10] R. A. Smith, Phys. Rev. A **43**, 1126 (1991).
[11] V. Berdichevsky, I. Kunin, and F. Hussain, Phys. Rev. A **43**, 2050 (1991).
[12] L. J. Campbell and K. O'Neil, J. Stat. Phys. **65**, 495 (1991).
[13] W. H. Matthaeus *et al.*, Physica (Amsterdam) **51D**, 531 (1991); D. Montgomery *et al.*, Phys. Fluids A **4**, 3 (1992).
[14] G. F. Carnevale *et al.*, Phys. Fluids A **4**, 1314 (1992).
[15] G. F. Carnevale *et al.*, Phys. Rev. Lett. **66**, 2735 (1991); J. B. Weiss and J. C. McWilliams, Phys. Fluids A (to be published).
[16] S. Kida, J. Fluid Mech. **112**, 397 (1981).
[17] A. Pumir and E. Siggia, Phys. Fluids **30**, 1606 (1987).
[18] H. Zirin, *Astrophysics of the Sun* (Cambridge Univ. Press, Cambridge, 1988).
[19] A. Pouquet, J. Fluid Mech. **88**, 1 (1978).
[20] D. Biskamp and H. Welter, Phys. Fluids B **2**, 1787 (1990), and references therein.
[21] W. M. Elsasser, Phys. Rev. **79**, 183 (1950).
[22] S. F. Edwards and J. B. Taylor, Proc. R. Soc. London A **336**, 257 (1974).
[23] S. E. Seyler, Jr., Phys. Fluids **19**, 1336 (1976).
[24] R. Jha *et al.*, Phys. Rev. Lett. **69**, 1375 (1992).
[25] W. W. Lee and H. Okuda, J. Comput. Phys. **26**, 139 (1978).